Generalization of Ionic Partition Diagrams to Lipophilic Compounds and to Biphasic Systems with Variable Phase Volume Ratios

Véronique Gobry,*,† Sorina Ulmeanu,† Frédéric Reymond,† Géraldine Bouchard,‡ Pierre-Alain Carrupt,‡ Bernard Testa,‡ and Hubert H. Girault†

Contribution from the Laboratoire d'électrochimie, École Polytechnique Fédérale de Lausanne, CH-1015 Lausanne, Switzerland, and Institut de Chimie Thérapeutique, Université de Lausanne, CH-1015 Lausanne, Switzerland

Received March 30, 2001. Revised Manuscript Received August 9, 2001

Abstract: The ionic partition diagram methodology has been generalized to address both hydrophilic and lipophilic compounds and to consider biphasic systems with variable phase volume ratios. With this generalized approach electrochemical measurements of ion transfer potentials afford the determination of the standard partition coefficients of all forms of ionizable molecules, including the neutral form, as well as the evaluation of the dissociation constant of monoprotic substances. An interesting consequence of this approach is the definition of an extraction $pK_{a,ext}$ which is the apparent pK_a of neutral acids and bases when dissolved in the organic phase.

1. Introduction

The distribution in biphasic liquid systems is an important aspect of many physicochemical and biological processes such as solvent extraction, analysis with ion selective electrodes, and pharmacokinetic distribution of drugs and other xenobiotics.

Ionic partition diagrams provide a useful representation of thermodynamic equilibria involving ionizable species in biphasic liquid systems. On the basis of Pourbaix diagrams for redox species,[1] these potential-pH diagrams[2] show schematically the predominance area of neutral and ionic species according to their acidic/basic character.[3] Initial studies of hydrophilic compounds by cyclic voltammetry at the interface between two immiscible electrolyte solutions (ITIES)[4−9] provided an accurate determination of their transfer potentials from one liquid phase to the other, thus allowing the determination of the standard partition coefficients of ionic species from their formal transfer potentials. These standard ionic partition coefficient values were then used to draw the boundary lines in ionic partition diagrams.[10−12] More recent studies involving lipophilic solutes such as *N*-(*p*-methylbenzyl)hexylamine[13] and Sildenafil[14] have shown that the experimental half-wave transfer potential values measured by an electrochemical method did not correspond directly to the boundary lines. This discrepancy has been ascribed to the fact that in the experiments the neutral species resided mainly in the organic phase whereas the ionic partition diagrams were drawn assuming that the neutral species were predominantly in the aqueous phase. To overcome this limitation, we propose here an extension of ionic partition diagrams for lipophilic compounds. This novel approach gives the opportunity to introduce the notion of extraction dissociation constant, which is the value to consider for extracting the solute from the organic to the aqueous phase.

Measuring the ion transfer reactions from water to the organic phase is a major experimental difficulty when dealing with lipophilic solutes. To ensure that the aqueous phase is at equilibrium, one must work with large phase volume ratios (V^o/V^w). To this end, a new cell has been designed and is described here.

To further expand the applicability of ionic partition diagrams, we propose here a generalized equipartition presentation involving number of moles rather than concentration, valid for both hydrophilic and lipophilic compounds.

2. Theory

2.1. The Case of a Lipophilic Monobasic Compound. When two immiscible phases α and β are brought into contact, a Galvani potential difference is established across the interface,

† École Polytechnique Fédérale de Lausanne.

‡ Université de Lausanne.

(1) Pourbaix, M. *Atlas d'Equilibres Electrochimiques*; Gautier-Villars: Paris, 1963.

(2) Reymond, F.; Steyaert, G.; Carrupt, P.-A.; Testa, B.; Girault, H. H. *J. Am. Chem. Soc.* **1996**, *118*, 11951−11957.

(3) Chopineaux Courtois, V.; Reymond, F.; Bouchard, G.; Carrupt, P.-A.; Testa, B.; Girault, H. H. *J. Am. Chem. Soc.* **1999**, *121*, 1743−1747.

(4) Kontturi, K.; Murtomaki, L. *J. Pharm. Sci.* **1992**, *81*, 970−975.

(5) Samec, Z.; Langmaier, J.; Trojanek, A.; Samcova, E.; Malek, J. *Anal. Sci.* **1998**, *14*, 35−41.

(6) Senda, M.; Kakiuchi, T.; Osakai, T. *Electrochim. Acta* **1991**, *36* (2), 253−262.

(7) Kubota, Y.; Katano, H.; Maeda, K.; Senda, M. *Electrochim. Acta* **1998**, *44*, 109−116.

(8) Kubota, Y.; Katano, H.; Senda, M. *Anal. Sci.* **2001**, *17*, 1−6.

(9) Senda, M.; Kubota, Y.; Katano, H. Voltammetric study of drugs at liquid−liquid interfaces. In *Liquid interfaces in chemical, biological, and pharmaceutical applications*; Volkov, A., Ed.; Marcel Dekker: New York, 2001; pp 683−698.

(10) Reymond, F.; Steyaert, G.; Carrupt, P.-A.; Testa, B.; Girault, H. H. *Helv. Chim. Acta* **1996**, *79*, 101−117.

(11) Reymond, F.; Carrupt, P. A.; Testa, B.; Girault, H. H. *Chem. Eur. J.* **1999**, *5*, 39−47.

(12) Reymond, F. Transfer mechanisms and lipophilicity of ionizable drugs. In *Liquid interfaces in chemical, biological, and pharmaceutical applications*; Volkov, A., Ed.; Marcel Dekker: New York, 2001; pp 729−774.

(13) Reymond, F.; Chopineaux Courtois, V.; Steyaert, G.; Bouchard, G.; Carrupt, P.-A.; Testa, B.; Girault, H. *J. Electroanal. Chem.* **1999**, *462*, 235−250.

(14) Gobry, V.; Bouchard, G.; Carrupt, P.-A.; Testa, B.; Girault, H. H. *Helv. Chim. Acta* **2000**, *83*, 1465−1474.

10.1021/ja015914f CCC: $20.00
Published on Web 10/04/2001

due to the partition of the charge carriers between the two adjacent phases:

$$\Delta_{\beta}^{\alpha}\phi = \phi^{\alpha} - \phi^{\beta} \tag{1}$$

where ϕ is the Galvani potential of the respective phase.

The electrochemical potential of a species i in phase α can be written as the sum of a chemical and an electrical term:

$$\tilde{\mu}_i^{\alpha} = \mu_i^{o,\alpha} + RT\ln a_i^{\alpha} + z_i F\phi^{\alpha} \tag{2}$$

where F is the Faraday constant, $\mu_i^{o,\alpha}$ is defined as the standard chemical potential, z_i is the charge, and a_i^{α} is the activity of species i.

At equilibrium, the electrochemical potentials of any species i distributed between two phases α and β are equal and the Galvani potential difference yields:

$$\Delta_{\beta}^{\alpha}\phi = \Delta_{\beta}^{\alpha}\phi_i^o + \frac{RT}{z_i F}\ln\left(\frac{a_i^{\beta}}{a_i^{\alpha}}\right) \tag{3}$$

with $\Delta_{\beta}^{\alpha}\phi_i^o = \Delta G_{tr,i}^{0,\alpha\rightarrow\beta}/z_i F$ defined as the standard potential of transfer of species i. Equation 3 is the Nernst equation, which describes the partition of the ionized form of a solute. When dealing with dilute solutions, eq 3 reduces to:

$$\Delta_{\beta}^{\alpha}\phi = \Delta_{\beta}^{\alpha}\phi_i^o + \frac{RT}{z_i F}\ln\left(\frac{c_i^{\beta}}{c_i^{\alpha}}\right) \tag{4}$$

When an ionizable solute is added to one of the two phases, a thermodynamic equilibrium is established that depends on the ability of the compound to dissociate, on the affinity of the different forms of this species for the two solvents, and on the ratio of the phase volumes. To model the partition of ionizable solutes, we have introduced earlier the concept of ionic partition diagrams, which consists of a representation of the area of predominance of the various species of a given ionizable solute as a function of pH and Galvani potential difference. Two adjacent areas of predominance are separated by equiconcentration boundary lines.

In such 2D plots, only one concentration of the neutral species can be displayed. Our early work was dedicated to the study of hydrophilic solutes, and the concentration of the neutral species in the aqueous phase (w) was originally chosen as the variable.[2] Thus, for a base B, only the area of predominance of the neutral base in water (B^{w}) appeared on the diagram as shown in Figure 1A. For lipophilic molecules, the concentration of the neutral species in the aqueous phase is small compared to that in the organic phase (o), and ionic partition diagrams displaying the neutral species in water are poorly relevant. The model has now been modified by taking into account the neutral base in the organic phase (B^{o}) when deriving the equations which define the boundary lines.

For a lipophilic monobasic compound B ($\log P_B^o > 0$) partitioning between two immiscible phases, the first boundary line (line 1 Figure 1B) corresponds to the equiconcentration of the two charged species BH^{+w} and BH^{+o}, as defined by the Nernst equation for ion transfer (eq 4) which reduces to:

$$\Delta_o^w\phi = \Delta_o^w\phi_{BH^+}^o \tag{5}$$

where $\Delta_o^w\phi_{BH^+}^o$ is the standard transfer potential of cation BH^+.

Two other boundaries have to be considered in the next step. The interfacial acidic/basic equilibrium between the charged species in the aqueous phase and the neutral species in the organic phase corresponds to the reaction:

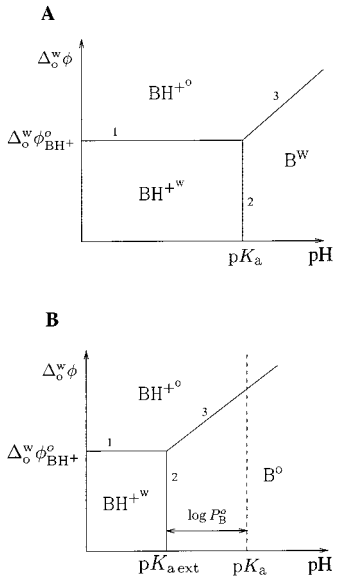

Figure 1. (A) Theoretical ionic partition diagram for a hydrophilic monobasic compound (equiconcentration convention). Lines 1, 2, and 3 are the equiconcentration boundary lines. (B) Theoretical ionic partition diagram for a lipophilic base (equiconcentration convention). The dotted line shows the value of the aqueous dissociation constant.

$$B^o + H_2O \rightleftharpoons BH^{+w} + OH^{-w}$$

The acidity constant in water can be expressed as a function of pH, the standard partition coefficient of B ($P_B^o = a_B^o/a_B^w$), and the ratio $a_B^o/a_{BH^+}^w$:

$$K_a^w = \frac{a_B^w \cdot a_{H^+}^w}{a_{BH^+}^w} = \frac{a_B^o}{a_{BH^+}^w}\cdot\frac{a_{H^+}^w}{P_B^o} \tag{6}$$

or

$$pK_a^w = -\log\left(\frac{a_B^o}{a_{BH^+}^w}\right) + pH + \log P_B^o \tag{7}$$

At low concentrations where activity coefficients can be neglected, the boundary line corresponding to equal concentrations of aqueous BH^{+w} and neutral base in the organic phase B^o (line 2 Figure 1B) is then given by:

$$pH = pK_a^w - \log P_B^o \tag{8}$$

This pH value can be considered as the extraction acidity constant $pK_{a,ext}$, since when using an aqueous acid to extract a neutral base from the organic phase, it is necessary to use a stronger acid than suggested by the aqueous bulk pK_a^w value. Indeed, $pK_{a,ext}$is lower than pK_a^w by one unit of pK_a per unit of $\log P_B^o$.

The boundary between BH^{+o} and B^o (line 3 Figure 1B) is similarly defined by developing the ratio $a_{BH^+}^o/a_B^o$ from the partition coefficients of the neutral and the Nernst eq 3 for BH^+ which reads:

$$\Delta_o^w\phi = \Delta_o^w\phi^o_{BH^+} + \frac{2.3RT}{F}\log\left(\frac{a^o_{BH^+}}{a^w_{BH^+}}\right) = \Delta_o^w\phi^o_{BH^+} + \frac{2.3RT}{F}\log P_{BH^+} \quad (9)$$

The partition coefficient P_{BH^+} is a function of the Galvani potential difference, itself established by the partition coefficient of all the other ionic species present in the biphasic system at equilibrium or imposed by the electrochemical setup when dealing with voltammetric experiments. Thus, by substitution of eq 6, eq 9 can be rewritten as:

$$\Delta_o^w\phi = \Delta_o^w\phi^o_{BH^+} + \frac{2.3RT}{F}\log\left(\frac{a^o_{BH^+}}{a^o_B}\right) + \frac{2.3RT}{F}\log\left(\frac{P^o_B K^w_a}{a^w_{H^+}}\right) \quad (10)$$

For dilute solutions, the boundary line between the neutral B^o and the charged species BH^{+o} in the organic phase is given by:

$$\Delta_o^w\phi = \Delta_o^w\phi^o_{BH^+} + \frac{2.3RT}{F}(\log P^o_B - pK^w_a) + \frac{2.3RT}{F}pH \quad (11)$$

Again, this boundary line is pH dependent.

Finally, the corresponding ionic partition diagram can be established as presented in Figure 1B. This figure shows that the more lipophilic the neutral base B, the smaller the predominance area of BH^+in water and the larger the predominance area of B in the organic phase.

2.2. The Case of a Lipophilic Monoacidic Compound. The case of a hydrophilic monoacid AH is shown in Figure 2A. In the case of a lipophilic monoacid AH a comparable thermodynamic development leads to the following equations for the three equiconcentration boundary lines:

Line 1:

$$\Delta_o^w\phi = \Delta_o^w\phi^o_{A^-} \quad (12)$$

Line 2:

$$pH = pK^w_a + \log P^o_{AH} \quad (13)$$

Line 3:

$$\Delta_o^w\phi = \Delta_o^w\phi^o_{A^-} - \frac{2.3RT}{F}(\log P^o_B + pK^w_a) + \frac{2.3RT}{F}pH \quad (14)$$

The corresponding ionic partition diagram is presented in Figure 2B. Again, the more lipophilic the acid AH, the smaller the predominance area of A^{-w}, and the larger the predominance area of AH^o.

Similarly, to extract a lipophilic acid AH from the organic phase, it is necessary to use a stronger base than suggested by the aqueous bulk pK_a value, i.e., one unit of pK_a larger per unit of log P^o_{AH} defining in this way an extraction pK_a value.

2.3. Phase Ratio Dependent Ionic Partition Diagrams Calculated in Number of Moles Rather Than Concentrations. We present below a more universal method to derive ionic partition diagrams valid for both hydrophilic and lipophilic neutral compounds, and based on a phase ratio dependent representation in terms of number of moles rather than concentrations. In this way, it becomes possible to take into account the total number of moles of a given neutral solute distributed between two phases.

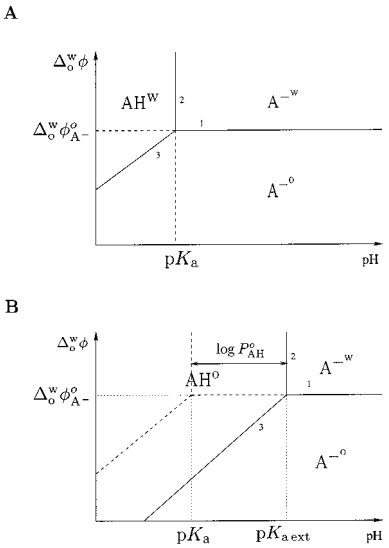

Figure 2. (A) Theoretical ionic partition diagram for a hydrophilic monoacidic compound (equiconcentration convention). (B) Theoretical ionic partition diagram for a lipophilic acid (equiconcentration convention). The dotted lines recall the corresponding ionic partition diagram 2-A for the corresponding hydrophilic acid.

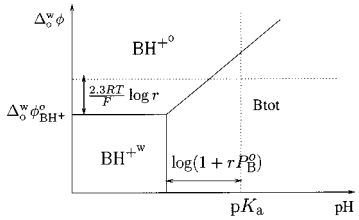

Figure 3. Ionic partition diagram calculated in number of moles for a monobasic compound (equipartition convention). The dotted lines show the corresponding pK_a and the $\Delta_o^w\phi^o_{BH^+}$ values.

For ideal solutions, the protonation equilibrium can be simplified and rewritten as:

$$K_a = \frac{c^w_B a^w_{H^+}}{c^w_{BH^+}} = \frac{n^w_B a^w_{H^+}}{n^w_{BH^+}} \quad (15)$$

where n^w_i is the number of moles of species i in the aqueous phase.

Let us first define the total number of neutral moles in the system, n_{Btot}, and the phase volume ratio, r, as:

$$n_{Btot} = n^w_B + n^o_B \quad (16)$$

and

$$r = \frac{V^o}{V^w} \quad (17)$$

It follows that the ratio of the number of moles of BH^+ is given by:

$$\frac{n^o_{BH^+}}{n^w_{BH^+}} = \frac{V^o c^o_{BH^+}}{V^w c^w_{BH^+}} = r\exp\left[\frac{F}{RT}(\Delta_o^w\phi - \Delta_o^w\phi^o_{BH^+})\right] \quad (18)$$

and the equation of the boundary line defined by $n^o_{BH^+} = n^w_{BH^+}$ (line 1 Figure 3) is:

$$\Delta_o^w\phi = \Delta_o^w\phi^o_{BH^+} - \frac{2.3RT}{F}\log r \qquad (19)$$

Similarly, substituting the terms of the partition coefficient of the neutral and charged species (eq 9) into the definition of the acidity constant in water leads to:

$$\frac{n_{B_{tot}}}{n^w_{BH^+}} = \frac{K_a}{a^w_{H^+}}(1 + rP^o_B) \qquad (20)$$

Therefore, when $n^w_{BH^+} = n_{B_{tot}}$ (line 2 Figure 3) we obtain:

$$pH = pK_a - \log(1 + rP^o_B) \qquad (21)$$

Finally, the boundary between $BH^{+o}$and B_{tot} (line 3 Figure 3) simplifies to:

$$\Delta_o^w\phi = \Delta_o^w\phi^o_{BH^+} - \frac{2.3RT}{F}(pK_a - \log r) + \frac{2.3RT}{F}pH \qquad (22)$$

This line is both potential- and pH-dependent. The corresponding ionic partition diagram is presented in Figure 3. This diagram clearly shows that the predominance area of BH^{+w} decreases as the phase ratio increases.

For a monoacid AH, it is straightforward to show that the boundary lines are expressed by equations similar to those for a monobase. The boundary line equation defined by $n^o_{A^-} = n^w_{A^-}$ (line 1 Figure 4) is:

$$\Delta_o^w\phi = \Delta_o^w\phi^o_{A^-} + \frac{2.3RT}{F}\log r \qquad (23)$$

The pH value (line 2) is given by:

$$pH = pK_a + \log(1 + rP^o_{AH}) \qquad (24)$$

Some authors refer to this pH value as the apparent p$K_a$value.[15] The corresponding ionic partition diagram is presented in Figure 4.

Figures 1 and 2 are particular cases of Figures 3 and 4. Indeed, when $r = V^o/V^w = 1$ and P approaches zero, which corresponds to the case of a hydrophilic compound, Figure 3 reduces to Figure 1A and in turn Figure 4 reduces to Figure 2A. In contrast, when $r = V^o/V^w = 1$ and P is large (lipophilic compound), Figures 3 and 4 reduce respectively to Figures 1B and 2B.

The case $r = V^o/V^w \ll 1$ is of particular pharmacological signification, since it corresponds to the ratio of phases encountered by a drug as it distributes in the body and passes through numerous aqueous compartments separated by thin organic membranes made of phospholipid bilayers.

3. Materials and Methods

3.1. Chemicals. All aqueous solutions were prepared with deionized water from a Milli-Q system (Millipor Milli-Q. 185). The organic solvent, 1,2-dichloroethane (1,2-DCE) (Fluka), was used according to safety instructions.[16] The organic salts bis(triphenylphosphoranylidene) ammonium tetrakis(4-chlorophenyl) borate (BTPPATPBCl) and tetrapropylammonium tetrakis(4-chlorophenyl)borate (TPATPBCl) were obtained by metathesis of equimolar quantities of the corresponding salts, potassium tetrakis(4-chlorophenyl) borate (KTPBCl)(Lancaster) and bis-(triphenylphosphoranylidene) ammonium chloride (BTPPACl)-(Fluka) and tetrapropylammonium bromide (Fluka), respectively. All other chemicals were provided by Fluka.

(15) Avdeef, A. *Quant. Struct.-Act. Relat.* **1992**, *11*, 510−517.

(16) International program on chemical safety, 2nd, Geneva, 1995; Vol. 176, p 148.

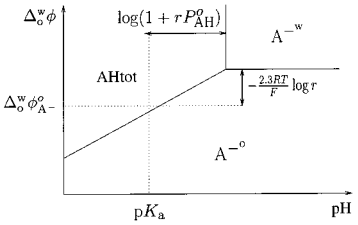

Figure 4. Ionic partition diagram calculated in number of moles for a monoacidic compound (equipartition convention). The dotted lines show the corresponding pK_a and the $\Delta_o^w\phi^o_{A^-}$ values.

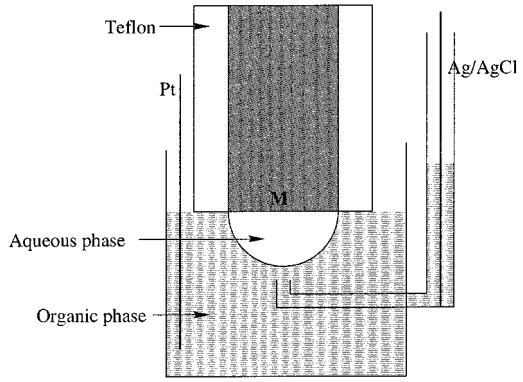

Figure 5. Schematic presentation of the droplet setup. M symbolizes the metal electrode

3.2. Electrochemical Methods. A 10 μL aqueous drop was laid on a metal disk electrode mounted in a Teflon holder. The aqueous phase consisted of a 10 mM solution of lithium chloride (LiCl). The electrode with its drop was then immersed in 2.5 mL of an organic electrolyte solution of BTPPATPBCl in 1,2-DCE. A platinum wire immersed in this organic phase acted as a counterelectrode, and a silver−silver chloride electrode immersed in an adjacent aqueous solution of 1 mM BTPPACl and 10 mM LiCl as the reference electrode.

Two kinds of disk electrodes can be used to support an aqueous droplet. First we used a platinum disk electrode together with the $Fe(SO_4)|Fe_2(SO_4)_3$redox couple in the aqueous phase at low pH.[17] The corresponding setup is presented in Figure 5.

The resulting electrochemical three-electrode cell is depicted by the following schematic representation where the double vertical bar represents the 1,2-dichloroethane|water interface.

Electrochemical Cell 1

		1mM BTPPACl	10 mM BTPPATPBCl	1 mM LiCl	
Ag	AgCl	10 mM LiCl	10 mM TPATPBCl	10 mM $FeSO_4$	Pt
				5 mM $Fe_2(SO_4)_3$	

Alternatively, a silver−silver chloride disk electrode can be used without restriction of the pH range. This silver−silver chloride disk electrode is prepared by oxidation of a silver disk electrode in an aqueous solution of NaCl containing a few drops of the corresponding concentrated acid. The three-electrode electrochemical cell corresponding to this setup is shown below

Electrochemical Cell 2

Ag	AgCl	1mM BTPPACl	5 mM BTPPATPBCl	10 mM LiCl	AgCl	Ag
		10 mM LiCl	0,2 mM TPATPBCl			

In both cases, the analyte should be placed in the organic phase to ensure complete equilibrium and the aqueous pH is controlled by adding either LiOH or HCl in the aqueous drop.

(17) Ulmeanu, S.; Lee, H.; Fermin, D.; Girault, H. H.; Shao, Y. *Electrochem. Commun.* **2001**, *3*, 219−223.

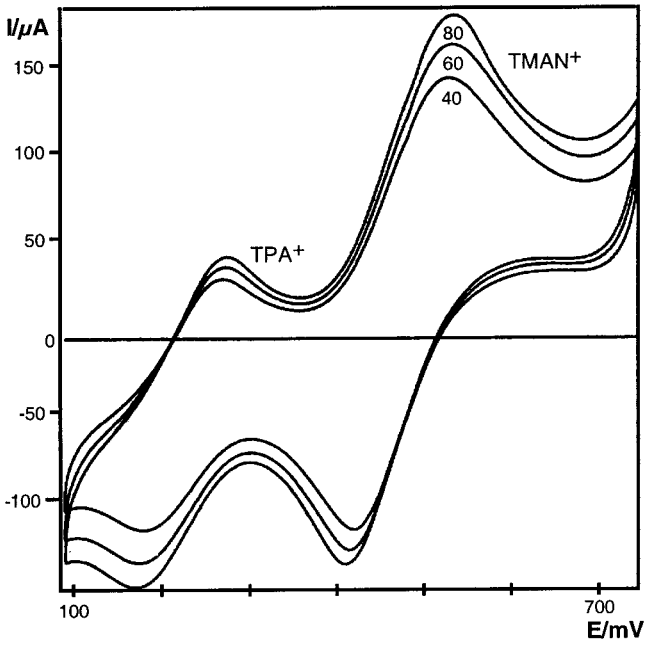

Figure 6. Cyclic voltammograms obtained for the transfer of 3,5-*N*,*N*-tetramethylaniline ($TMAN^+$) at three different scan rates (40, 60, 80) with the droplet system at pH 3. TPATPBCl is added as internal reference according to Cell 2.

Cyclic voltammetry was carried out by using a 3-electrode potentiostat equipped with *IR* compensation and connected to an *X*−*Y* recorder. Compared to a large interface setup as used previously,[2] the main advantage of the present droplet system is the short time needed to reach equilibrium between the two phases when studying lipophilic compounds.

4. Results and Discussion

4.1. Ionic Partition Diagrams Based on the Equiconcentration Convention of a Lipophilic Monobasic Compound (3,5-*N*,*N*-Tetramethylaniline). The transfer of 3,5-*N*,*N*-tetramethylaniline was studied at various pH values. Ion transfer half-wave potentials were referred to the half-wave potential of the tetrapropylammonium (TPA) ion added at the end of the experiment in the organic phase as TPATPBCl salt. The analyte was added to the organic phase since the large volume ratio guaranteed a fast partition in water without altering its concentration in the organic phase. A typical cyclic voltammogram is shown in Figure 6.

The half-wave transfer potential measured by cyclic voltammetry as the mid-peak potential shifted with increasing pH. As illustrated by the resulting ionic partition diagram (Figure 7), increase of the transfer potential occurred before the aqueous dissociation constant value of 5.52 (value measured by potentiometry (pH-metric titration method[18])).

These results obtained by amperometry are in total agreement with the theory presented above, since the measured $pK_{a,ext}$ value of 1.8 yields a log P^o_B value of 3.7, which can be compared to the standard ion partition coefficient of the neutral 3,5-*N*,*N*-tetramethylaniline measured to be equal to 4.0 by potentiometry. This example clearly demonstrates how a series of electrochemical measurements of standard transfer potential yield the standard partition coefficients of both the neutral base and the protonated form.

4.2. Ionic Partition Diagram in the Equiconcentration Convention of a Lipophilic Monoacidic Compound (2,4-Dinitrophenol). To validate the theory developed above for a monoacid, we studied the lipophilic monoacid 2,4-dinitrophenol (2,4-DNP). Given the aqueous dissociation constant ($pK_a = 4.1$) and the partition coefficient (log $P^o_{AH} = 2.6$) of this solute,[3] the above theory predicted an effective $pK_{a,ext}$ value of 6.7. The ionic partition diagram reported in Figure 8 confirms this prediction.

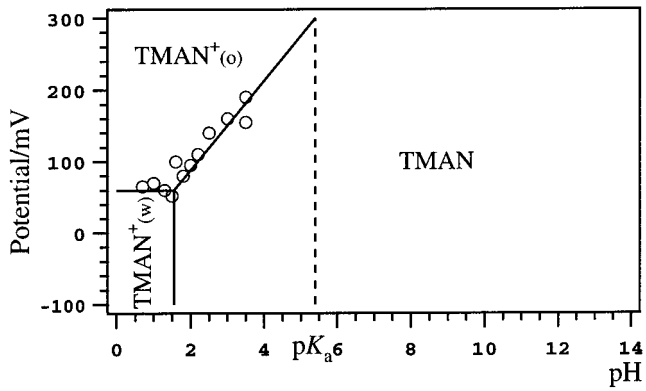

Figure 7. Ionic partition diagrams of 3,5-*N*,*N*-tetramethylaniline with the droplet system (equiconcentration convention) ($c^o_{TMAN}/c^w_{TMAN} = 1$, 66×10^4). The dotted line shows the pK_a value.

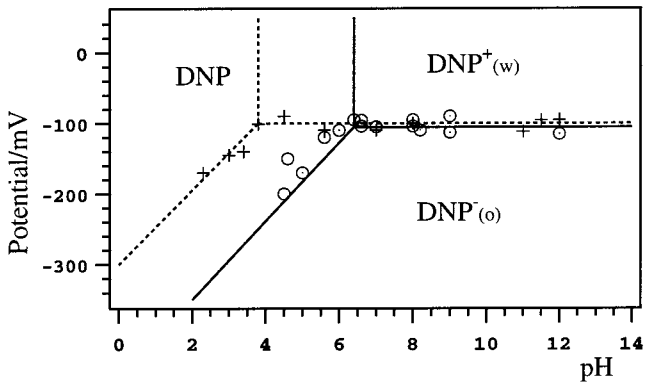

Figure 8. Ionic partition diagrams of 2,4-dinitrophenol ($c^o_{TMAN}/c^w_{TMAN} = 4 \times 10^2$) obtained with both the droplet electrochemical cell (unbroken line and circles) and the large interface four-electrode cell (dotted line and crosses, data taken from ref 3) (equiconcentration convention).

For both a lipophilic base and acid, the main change in the ionic partition diagram compared to previous representations is an enlargement of the area corresponding to the neutral species. In both cases, the neutral form in the organic phase is the predominant species since it occupies the largest pH area. Charged forms exist in the low and high pH values, respectively, acidic pH values for a basic compound, and basic pH values for an acidic compound.

4.3. Ionic Partition Diagrams Based on Equipartition (Same Number of Moles in Both Phases). Ionic partition diagrams expressing number of moles rather than concentrations were plotted according to the above theory for the two investigated compounds (Figures 9 and 10).

These diagrams, calculated from the experimentally derived Figures 7 and 8, provide additional information on the partition process. The large phase volume ratio ($r = 250$) enlarges even further the predominance area of the neutral species which, for the lipophilic compounds investigated, corresponds to that of the neutral species in the organic phase.

For 3,5-*N*,*N*-tetramethylaniline between pH 0 and 14, the overall majority of molecules are in the neutral form. As a consequence, in this pH range, the compound was present only

(18) Avdeef, A.; Comer, J. *QSAR Mol. Modelling* 1993, 386−387.

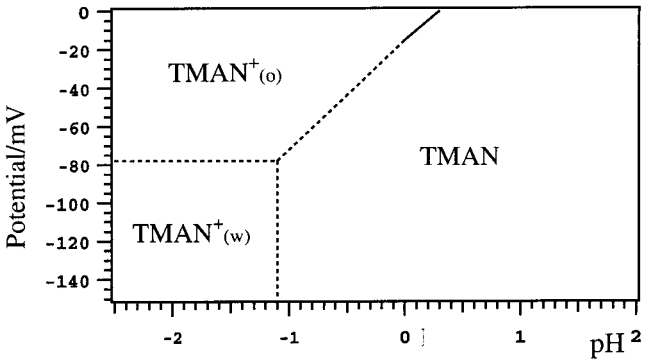

Figure 9. Ionic partition diagram of 3,5-*N*,*N*-tetramethylaniline (equipartition convention). The dotted line corresponds to values for pH ≪0.

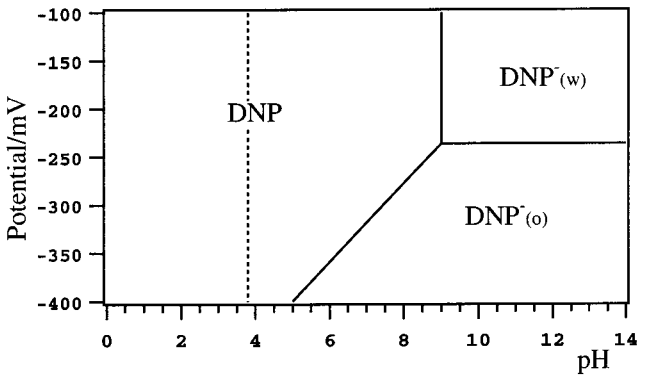

Figure 10. Ionic partition diagram of 2,4-dinitrophenol (equipartition convention).

in the organic phase, and would only be present in the aqueous phase at pH ≪−1.1, where the cationic form would predominate.

In the case of 2,4-dinitrophenol, the compound was also in its neutral form at most pH values. The compound also exists in its anionic form in the organic phase above pH 5, and it partitions between the two phases in charged form for pH higher than 9.

In both pH regions, the compound is present in the organic phase mostly in its neutral form, clearly suggesting that the neutral species will permeate easily across biomembranes due to the displacement of the pK_a value caused by the positive log P^o_{AH} value and the phase volume ratio. Figure 10 is therefore useful to explain the uncoupling activity of DNP on the cellular energy production.[3]

4.4. Transfer Mechanisms. The difference existing between hydrophilic and lipophilic compounds in the predominance area of their various species is also related to the interfacial transport processes at the various boundary lines. In fact, as shown above, the electrochemical methodology is an efficient tool to study interfacial acid−base reactions, but it is important to distinguish between the different mass transfer controlled reactions.

In the equiconcentration convention, the boundary line that corresponds to the partition of the charged species between the two adjacent phases (lines 1, Figures 1 and 2) remains unchanged whether one considers a hydrophilic or a lipophilic compound. A lipophilic cation BH^+ is characterized by a negative standard transfer potential ($\Delta^w_o\phi^o_{BH^+} \ll 0$) whereas a hydrophilic cation is characterized by a positive standard transfer potential ($\Delta^w_o\phi^o_{BH^+} \gg 0$). A lipophilic anion A^- is characterized by a positive standard transfer potential ($\Delta^w_o\phi^o_{A^-} \gg 0$), whereas

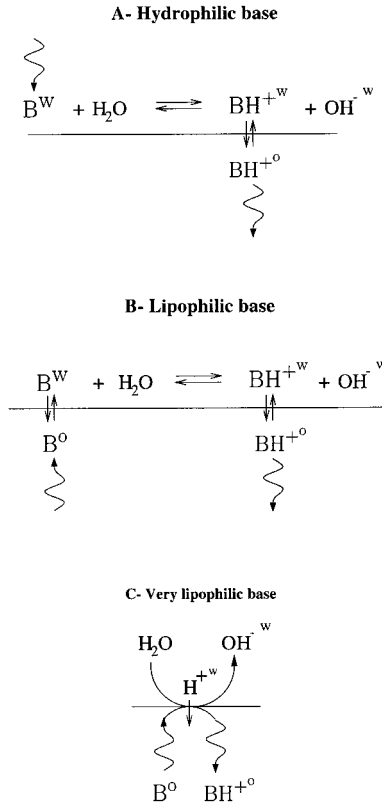

Figure 11. Transfer mechanisms in assisted proton transfer for a hydrophilic base and a lipophilic base. The winding arrow illustrates the diffusion process from the bulk to the interface.

a hydrophilic anion is characterized by a negative standard transfer potential ($\Delta^w_o\phi^o_{A^-} \ll 0$).

Line 2 is related to the aqueous acid/base equilibrium which, in the case of a hydrophilic neutral compound, is not affected by the presence of the organic phase. In the case of a lipophilic neutral molecule, we are now dealing with heterogeneous acid/base equilibria which can be written as follows: for a lipophilic acidic molecule, it can be written for a base as:

$$B^o + H_2O \rightleftharpoons BH^{+w} + OH^{-w}$$

and for a lipophilic acidic molecule as:

$$A^{-w} + H^{+w} \rightleftharpoons AH^o$$

Both cases are related to the extraction of a neutral molecule upon pH variations. This type of reaction cannot be studied by electrochemical methods. Line 2 is therefore obtained by extrapolation of lines 1 and 3.

The transfer mechanisms connected with the third boundary line (3) can be classified in the following way:

(a) For an hydrophilic base (Figure 11A), the reaction is:

$$B^w + H_2O \rightleftharpoons BH^{+o} + OH^{-w}$$

The corresponding boundary line 3 in Figure 1A is given by the following equation:[2]

$$\Delta^w_o\phi = \Delta^w_o\phi^o_{BH^+} - \frac{2.3RT}{F}pK_a + \frac{2.3RT}{F}pH \qquad (25)$$

From an experimental viewpoint, using a classical electrochemical cell for the study of ion transfer reactions,[3] the hydrophilic base is dissolved in water and the transfer of BH^+

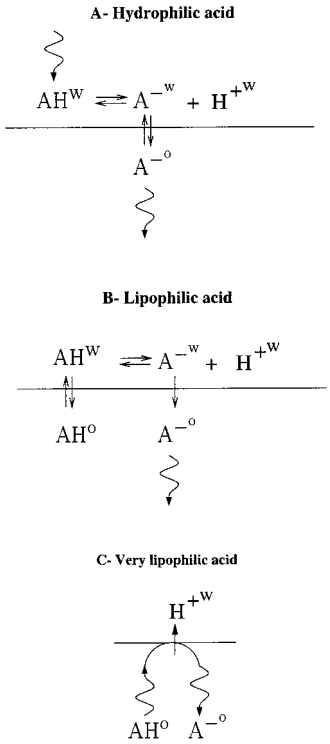

Figure 12. Distribution profiles and connected proton-transfer mechanisms for a hydrophilic acid and a lipophilic acid. The winding arrow illustrates the diffusion process from the bulk to the interface.

from water to oil is observed electrochemically. Because the dissociation of water is a very fast reaction, the ion transfer reaction is controlled by the diffusion of B^w in water and that of BH^{+o} in oil since the other reactants, namely water and OH^{-w}, are in excess. This type of experiment is best carried out in systems having a small phase ratio (V^o/V^w).

(b) For a hydrophilic acid (Figure 12A) the reaction is:

$$AH^w \rightleftharpoons A^{-o} + H^{+w}$$

(Figure 12), and the boundary line 3 in Figure 2A is given by

$$\Delta_o^w\phi = \Delta_o^w\phi^o_{A^-} + \frac{2.3RT}{F}pK_a + \frac{2.3RT}{F}pH \qquad (26)$$

As above, from an experimental point of view, the hydrophilic acid is dissolved in water and the transfer of A^- from water to oil is observed electrochemically. Because the acid−base equilibrium in water is fast, the ion transfer reaction is controlled by the diffusion of AH in the aqueous phase and of A^- in the organic phase. Alternatively, we can synthesize by metathesis an organic salt made of the anion A^{-o} and a very lipophilic cation C^{+w} such as $BTPPA^+$.[3,19] In this way, it becomes possible to observe the transfer of A^{-o} from oil to water, and back again in the reverse sweep when using cyclic voltammetry. The mass transfer is still limited by the diffusion of A^{-o} and AH^w. The proton is involved in this anion transfer as shown by the pH dependence of the half-wave potential.

(c) For a lipophilic base the reaction is:

$$B^o + H_2O \rightleftharpoons BH^{+o} + OH^{-w}$$

and the boundary line 3 in Figure 1B is given by eq 11.

Experimentally, the lipophilic base is dissolved in the organic phase of an electrochemical cell with a large phase ratio as shown in Figure 5. Upon application of a potential difference in the positive direction, a current corresponding to the transfer of BH^+ from water to oil is observed (Figure 6). Here, the process is limited by the diffusion of B^o from the organic phase to the interface, by the very fast protonation, and then by the diffusion of the protonated BH^{+o} to the organic phase away from the interface. For very lipophilic bases, the protonation reaction can be considered as an interfacial reaction, and this reaction is analogous to a reduction on a metallic electrode controlled by the diffusion of the oxidized species to the electrode, followed by a very fast electron transfer and then by the diffusion of the reduced species.

The half-wave potential for linear diffusion is then given by:

$$\Delta_o^w\phi^{1/2} = \left(\Delta_o^w\phi^{o'}_{H^+} + \frac{RT}{F}\ln P_B^o\right) + \frac{RT}{2F}\ln\left(\frac{D^o_{BH^+}}{D_B{}^o}\right) \qquad (27)$$

where D_B^o and $D^o_{BH^+}$ are the organic diffusion coefficients of the neutral and cationic species, respectively.

(d) For a lipophilic acid, the reaction is:

$$AH^o \rightleftharpoons A^{-o} + H^{+w}$$

The corresponding line 3 in Figure 2B is described by eq 14.

Once again, from an experimental point of view, the lipophilic acid is dissolved in the organic phase of an electrochemical cell with a large phase ratio (vide supra). The transfer of the proton released from oil to water is observed (Figure 11B). The process is limited by the diffusion of the two species involved, AH^o and A^{-o}. It may be worth explaining why the data for 2,4-dinitrophenol reported in a previous paper[3] yielded the points shown in Figure 8. These data were obtained with a large interface electrochemical cell, dissolving the solute in the aqueous phase in its anionic form, and decreasing the pH afterward. Such experimental conditions did not allow saturation equilibrium to be reached.

5. Conclusion

The present work shows that depending on the hydrophilic or lipophilic character of the solute, it is informative to measure electrochemically the half-wave transfer potentials of the ionized forms at different pH values in systems with appropriate phase volume ratios ($V^o \ll V^w$). Systems having a small phase ratio are adequate to study hydrophilic compounds, whereas systems having a large phase ratio lend themselves to the study of lipophilic compounds. Electrochemical methods such as cyclic voltammetric are able to yield directly both the standard ionic partition coefficient of the ionized species and the standard partition coefficient of the neutral species of a given compound. They also allow us to visualize the extraction $pK_{a,ext}$ of lipophilic compounds when plotting ionic partition diagrams calculated in the equiconcentration convention. The biological consequences of pK_a shifts and phase ratios are better deduced from a presentation of ionic partition diagrams calculated in number of moles and presented in an equipartition convention.

Acknowledgment. P.A.-C., H.H.G., and B.T. are grateful for financial support by the Swiss National Science Foundation.

JA015914F

(19) Ding, Z.; Reymond, F.; Baumgartner, P.; Fermin, D.; Brevet, P.-F.; Carrupt, P.-A.; Girault, H. H. *Electrochim. Acta* **1998**, *44*, 3.

(20) Volkov, A., Ed. *Liquid interfaces in chemical, biological, and pharmaceutical applications*; Marcel Dekker: New York, 2001.